

Strain-triggered high-temperature superconducting transition in two-dimensional carbon allotrope

Tian Yan¹, Ru Zheng¹, Jin-Hua Sun¹, Fengjie Ma², Xun-Wang Yan³, Miao Gao^{1,†}, Tian Cui^{1,‡}, Zhong-Yi Lu^{4,§}¹Department of Physics, School of Physical Science and Technology, Ningbo University, Zhejiang 315211, China²The Center for Advanced Quantum Studies and Department of Physics, Beijing Normal University, Beijing 100875, China³College of Physics and Engineering, Qufu Normal University, Shandong 273165, China and⁴Department of Physics, Renmin University of China, Beijing 100872, ChinaCorresponding authors. E-mail: [†]gaomiao@nbu.edu.cn, [‡]cuitian@nbu.edu.cn, [§]zlu@ruc.edu.cn

Received January 3, 2026; accepted April 8, 2026

Supporting Information

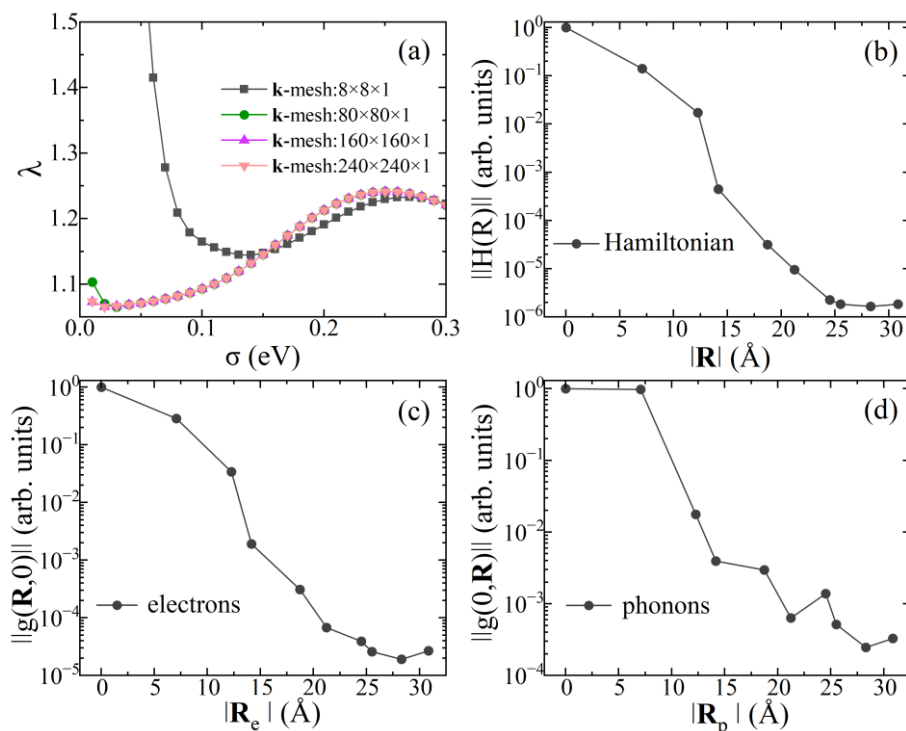


Figure S1. (a) Convergence test of EPC constant versus smearing parameter σ in THO-graphene under 12% strain. Fine phonon grid is chosen to be $80 \times 80 \times 1$. (b) Spatial decay of the electronic Hamiltonian in Wannier representation. (c) and (d) Spatial decays of EPC matrix elements in Wannier representation. Data in (b)-(d) are normalized by their respective maximum values.

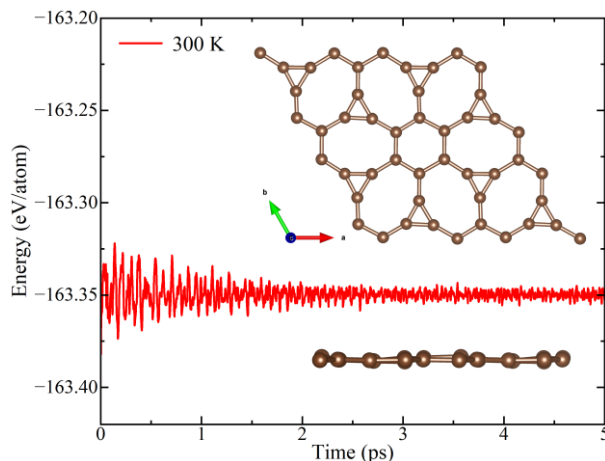


Figure S2. Time evolution of the total energy per atom in the THO-graphene at 300 K obtained in *ab initio* molecular dynamics. The insets show the top and side views of the final snapshot at 5 ps.

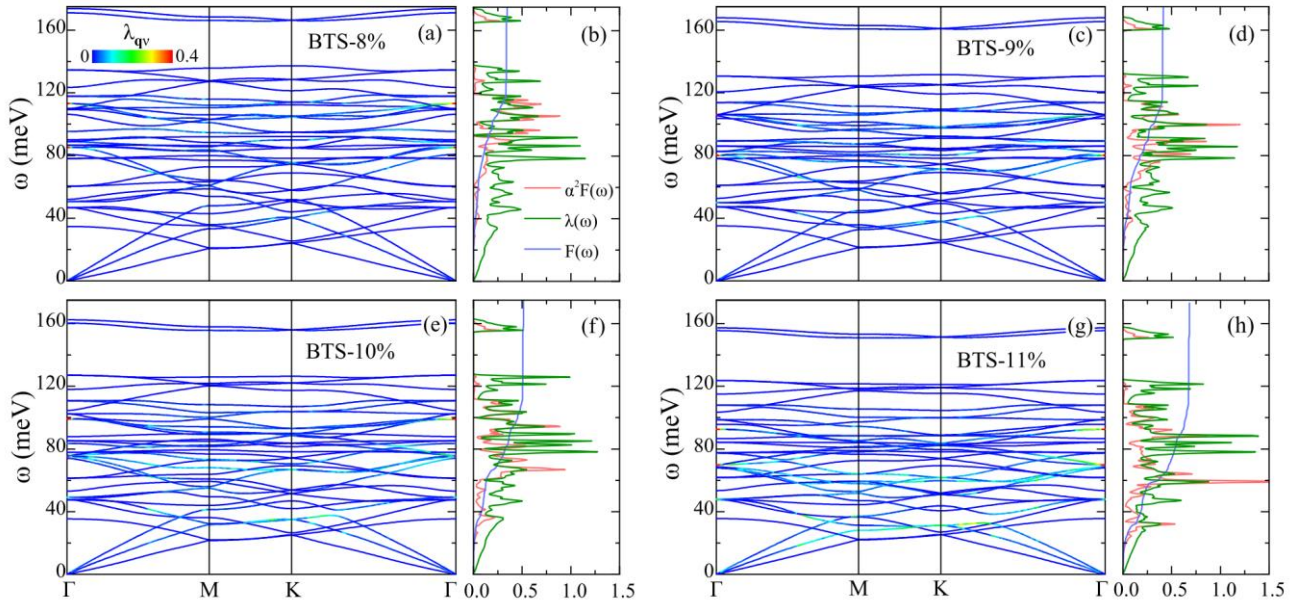


Figure S3. Lattice dynamics of THO-graphene under BTS of 8%, 9%, 10%, and 11%. (a), (c), (e), (g) Phonon spectra at different BTS. Colors represent the strength of EPC constant $\lambda_{q\nu}$ for phonon mode $q\nu$. (b), (d), (f), (h) Phonon density of states $F(\omega)$ (modes/meV), Eliashberg spectral functions $\alpha^2F(\omega)$ and $\lambda(\omega)$.

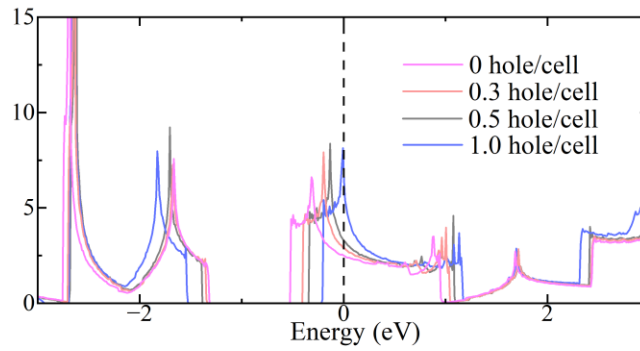


Figure S4. Density of states under different doping concentrations at BTS of 12%.

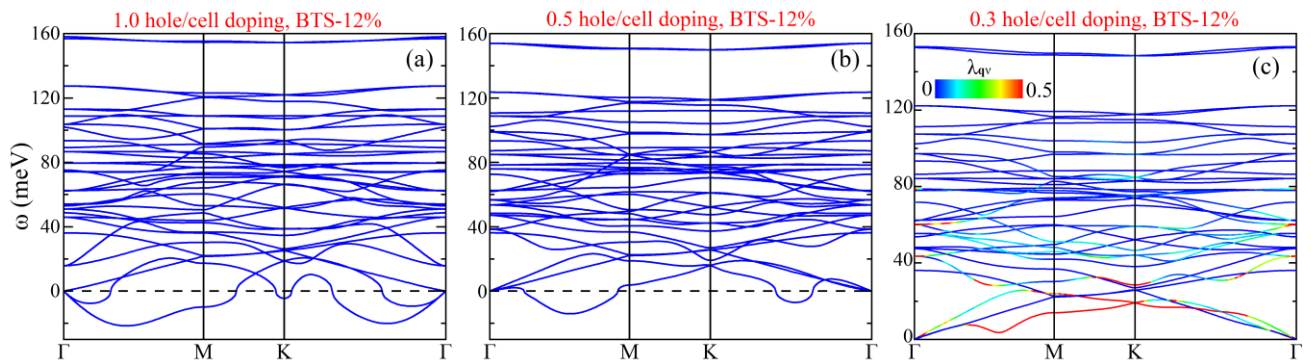


Figure S5. Phonon spectra at different doping concentrations under 12% BTS. The strengths of $\lambda_{q\nu}$ are mapped by different colors for 0.3 hole/cell doped THO-graphene.

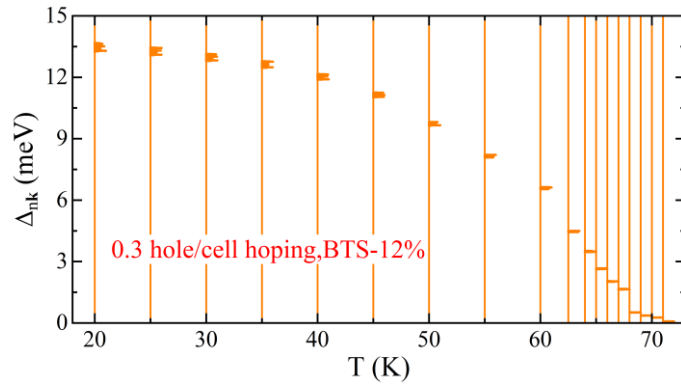


Figure S6. Temperature dependence of the superconducting gap Δ_{nk} under doping concentration of 0.3 hole/cell and 12% BTS.

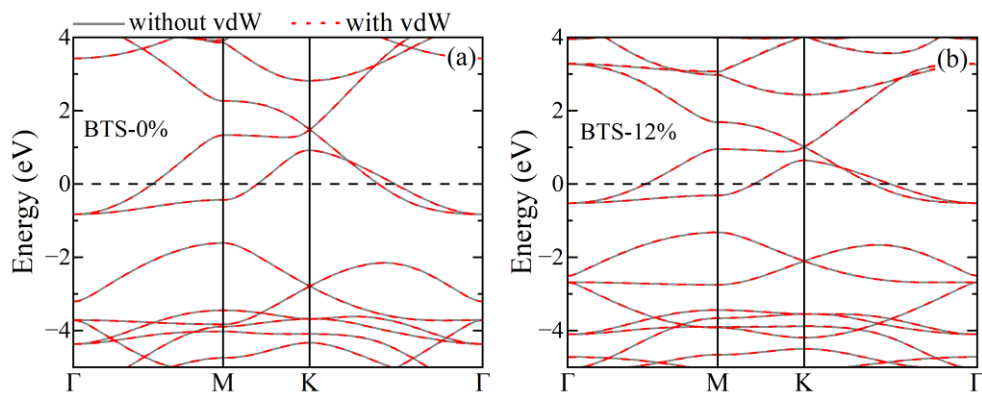


Figure S7. Band structures for the unstrained and 12%-strained THO-graphene with (dashed lines) and without (solid lines) vdW correction.

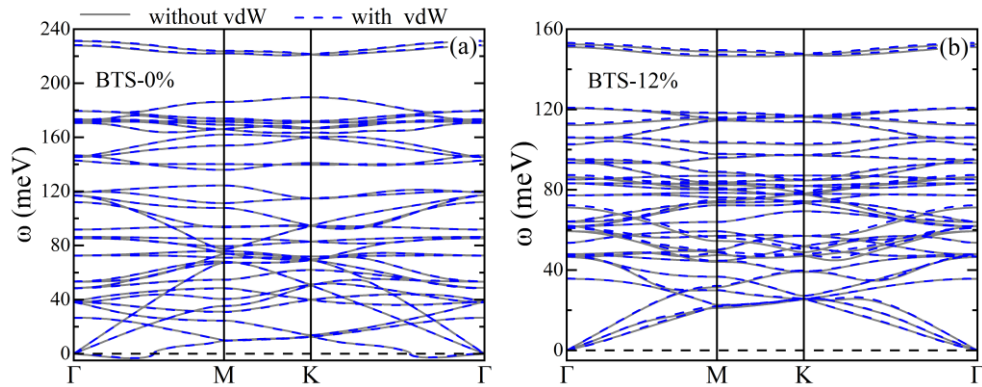


Figure S8. Phonon spectra for the unstrained and 12%-strained THO-graphene with (dashed lines) and without (solid lines) vdW correction.

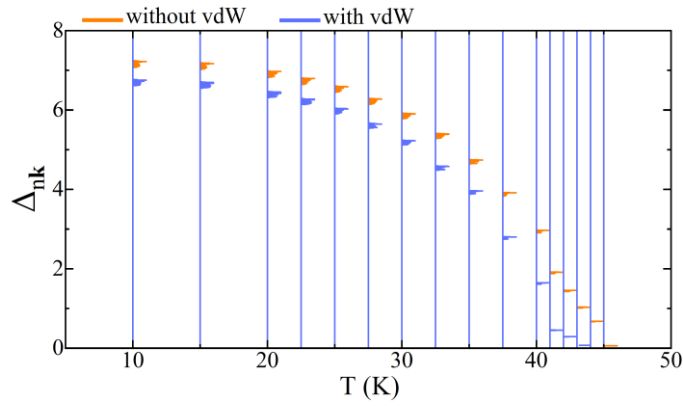


Figure S9. Superconducting gap distribution versus temperature under 12% strain. Orange and blue curves represent the results without and with vdW correction, respectively.

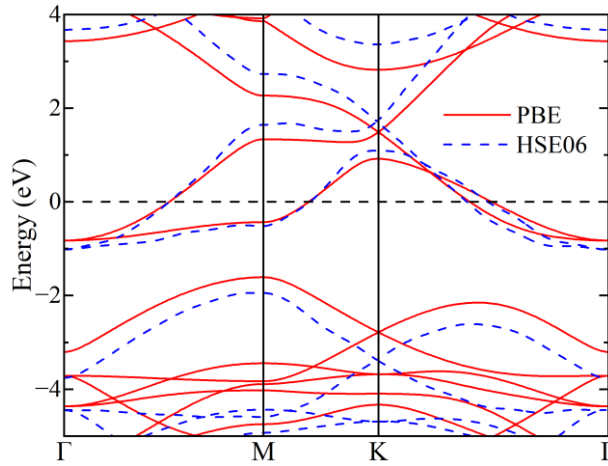


Figure S10. Band structure calculated with HSE06 hybrid functional for free-standing THO-graphene.

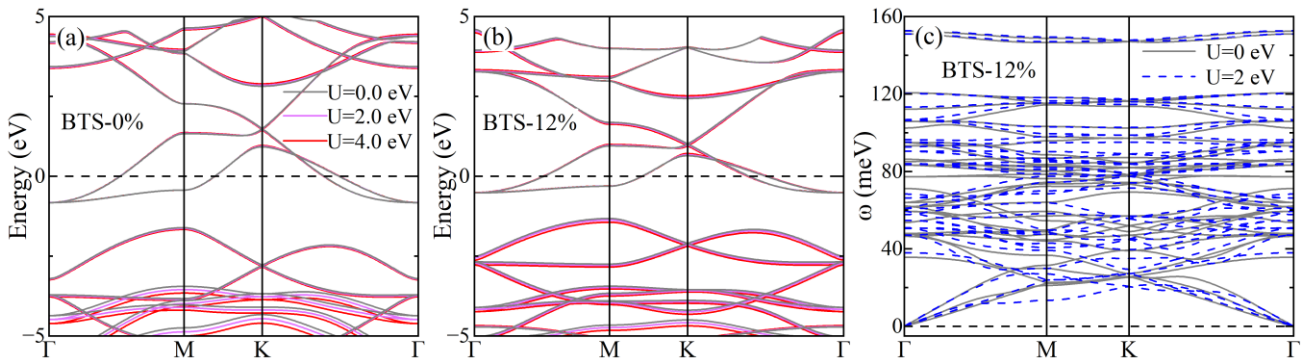


Figure S11. Influences of strong correlation on electronic structures and phonons of THO-graphene. Band structures of free-standing (a) and 12%-strained THO-graphene (b) under different U values. (c) Phonon spectra comparison for 12%-strained THO-graphene with and without the inclusion of $U=2.0$ eV.